

## Structure Functions in a Model of Turbulent Energy Dissipation

Jan Finjord<sup>1</sup>

*Received July 17, 1991; final December 11, 1991*

---

A stochastic activity-transfer model, previously proposed to apply to turbulence, is studied and simulated on a  $256 \times 256$  lattice. Introduction of random self-activation does not allow stable fronts to develop in the limit of small growth probability. By assigning discrete density values equal to the threshold values in a related continuous and deterministic model, the structure functions for distances  $r$  in the lattice are calculated. They have a functional form different from the power behavior which in the case of the deterministic version was interpreted as another sign of self-organized criticality. Future studies of these and other models may be facilitated by the algorithm developed for structure function calculations.

---

**KEY WORDS:** Scaling; forest-fire model; self-organized criticality; turbulence.

### 1. INTRODUCTION

An analogy between hydrodynamic turbulence and a "forest-fire" model on a lattice has been proposed.<sup>(1,2)</sup> The basic analogy would be that energy is injected statistically homogeneously and is dissipated on a fractal. A central assumption in the model is that self-organized criticality<sup>(3),2</sup> occurs in the limit of small tree growth probability (energy injection rate)  $p$ , a trait which would come about since the forest-fire model, like the original sandpile model, includes an element of metastability. Recently it has been claimed,<sup>(5,6)</sup> however, that the simulations of the forest-fire model do not show self-organized criticality: Instead, it was interpreted as being percolation-like, which should also be the behavior in the very limit  $p \rightarrow 0$  if criticality appears there.

---

<sup>1</sup> Rogaland University Center, Stavanger, Norway.

<sup>2</sup> See, e.g., ref. 4 for a recent review of the literature on self-organized criticality.

Also a modified two-dimensional model has recently been proposed to explain some generic properties of turbulence.<sup>(7)</sup> This model is deterministic, with a uniform tree density growth rate  $p$ , and occurrence of “trees” and also self-ignition as the density grows past thresholds (in addition to nearest-neighbour ignition). In this sense the model is continuous. An analogy with experimental results (and with the  $\beta$  model predictions) for turbulence<sup>(8)</sup> is indeed found<sup>(7)</sup>: The structure functions of the “tree” density  $n(\mathbf{x})$

$$S_q(r) = \langle |n(\mathbf{x}_0 + \mathbf{x}) - n(\mathbf{x}_0)|^q \rangle \quad (1)$$

with  $r - 1 < |\mathbf{x}| \leq r$  ( $r$  integer), were demonstrated by simulation to follow the scaling law

$$S_q \approx r^{\zeta(q)}, \quad \zeta(q) \approx 0.027q \quad (2)$$

for  $2 \leq q \leq 14$ , for small (but finite)  $p$  on a  $400 \times 400$  lattice. The  $\langle \cdot \rangle$  brackets in Eq. (1) denote an ensemble average. Furthermore, the model was shown to have zero Lyapunov coefficients and a power-law divergence of nearby trajectories (“weak chaos”). These scaling properties have been taken as another indication of self-organized criticality.

Concerning the criticality, there is thus disputed evidence in the discrete model, while the reported results in the continuous model are positive. Also, in ref. 7 an ergodicity assumption was used in the evaluation of the average in Eq. (1): Only one point for  $\mathbf{x}_0$  was used per time step<sup>(9)</sup> instead of an average over  $\mathbf{x}_0$  (apparently for computational reasons), with the need for a subsequent average over a large number of time steps (up to 40,000). A similar procedure was used for the calculation of number distributions in ref. 2, with limited accuracy as a result.

The present paper reports on work addressing the following topics, related to the above-mentioned problems:

1. Whether the scaling results for the structure functions of the continuous model carry over to the original (discrete) model.
2. Whether random self-ignition with probability  $p$  can be introduced in the discrete model.
3. Technically, whether it is feasible in practice to integrate over both space points in the average in (1).

A preliminary account of the results has been reported elsewhere.<sup>(10)</sup>

## 2. SIMULATIONS

### 2.1. The Model

We study the discrete model on a two-dimensional square lattice with periodic boundary conditions. To avoid a pyrotechnical terminology when the model is applied to turbulent states in general, we will call the sites “empty,” “filled,” or “active.” In this model we will assign density values equal to the threshold values in the continuous model, so that an empty site, a filled site, and an active site have the density values 0, 1, and 2, respectively. The lattice model rules are as follows:

1. An empty site becomes filled with probability  $p$  per time step.
2. Active sites become empty after one time step.
3. A filled site nearest-neighbor to an active site becomes active in the next time step.
4. Optionally, a filled site with no active neighbors can spontaneously become active with probability  $p$  per time step (self-activation).

The optional specification of random self-activation would on the average make a filled site self-activate after  $p^{-1}$  time steps if a statistically stationary state occurs, like what would be the self-ignition time delay in the deterministic continuous model.

For the time-step advancement in the model, and also for the number density calculations, we use lists<sup>(11)</sup> of sites activated or emptied in the previous time step. This speeds up the actual calculations considerably. For the calculations of the number density of active sites it allows for an average over all active sites taken as starting points, taking advantage of the periodic boundary conditions (limited, of course, to distances up to half the lattice size to avoid double-counting<sup>3</sup>).

For one time step (say, the  $k$ th) in the ensemble average, the structure functions are most simply computed by a double sum where the indices  $i$  and  $j$  both run over all lattice sites:

$$S_q^{(k)}(r) = \sum_i \sum_j P(r | \mathbf{x}_i, \mathbf{x}_j) | n_i^{(k)} - n_j^{(k)} |^q \tag{3}$$

The operator  $P(r | \mathbf{x}_i, \mathbf{x}_j)$  projects out pairs of sites with one site on a “shell” around the other, taken here as  $r - \frac{1}{2} < |\mathbf{x}_i - \mathbf{x}_j| \leq r + \frac{1}{2}$  ( $r$  integer). Periodic boundary conditions are used to find the shortest value of the difference between a given pair of vector components. The projection operator

<sup>3</sup> In ref. 7, structure functions have been plotted up to  $r$  values of 275–280, with  $N = 400$ .

is understood to include weights according to the number of points in a shell, as well as the factor due to the average over center points.

In the evaluation of the sums in Eq. (3), the CPU time requirement grows as  $N^{2d}$ , with  $d$  the dimensionality of the lattice and  $N$  the edge length. Performing such a feat for increasing  $N$  time step after time step would quickly become impractical also on supercomputers, even with obvious simplifications such as replacing square root calculations by table lookup and taking advantage of the symmetry of the sum.

## 2.2. A Fast Algorithm for the Structure Functions

For even  $q$  values, there is a way around the problem with the evaluation of the double sum in Eq. (3). It is applicable to all cases where a small fraction of the sites change their density value per time step. Introduce a matrix  $\Delta_i^{(k)}$  which keeps track of the changes in  $n_i$  since the previous time step:

$$n_i^{(k)} = n_i^{(k-1)} + \Delta_i^{(k)} \quad (4)$$

Then

$$S_q^{(k)}(r) = S_q^{(k-1)}(r) + T_q^{(k)}(r) \quad (5)$$

$$T_q^{(k)}(r) = \sum_i \sum_j P(r | \mathbf{x}_i, \mathbf{x}_j) \{ |n_i^{(k-1)} - n_j^{(k-1)} + \Delta_i^{(k)} - \Delta_j^{(k)}|^q - |n_i^{(k-1)} - n_j^{(k-1)}|^q \} \quad (6)$$

$$\begin{aligned} \frac{1}{K} \sum_{k=1}^K S_q^{(k)}(r) &= S_q^{(1)}(r) + \frac{K-1}{K} T_q^{(2)}(r) \\ &+ \frac{K-2}{K} T_q^{(3)}(r) + \dots + \frac{1}{K} T_q^{(K)}(r) \end{aligned} \quad (7)$$

The time average implied by the ensemble average will thus be fast if each  $T_q^{(k)}(r)$  can be computed efficiently. Observe that the summand in Eq. (6) is symmetric in the permutation of the indices  $i$  and  $j$ , and separate the index values into two groups  $\{\alpha\}$  and  $\{\beta\}$ :

$$i \in \{\alpha\} \Leftrightarrow \Delta_i^{(k)} = 0 \quad (8)$$

$$i \in \{\beta\} \Leftrightarrow \Delta_i^{(k)} \neq 0 \quad (9)$$

The possible  $i, j$  combinations in the sum in Eq. (6) are (because of the symmetry)

$$\{\alpha, \alpha\} \quad 2\{\alpha, \beta\} \quad \{\beta, \beta\} \quad (10)$$

whereas if the  $i$  sum were restricted to include only  $i \in \{\beta\}$  one would get

$$\{\alpha, \beta\} \quad \{\beta, \beta\} \tag{11}$$

Since the summand in Eq. (6) is proportional to  $\Delta_i^{(k)} - \Delta_j^{(k)}$  for even  $q$  values, contributions in the group  $\{\alpha, \alpha\}$  will all be zero since there all  $\Delta_i^{(k)} = 0$ . The double sum in Eq. (6) can thus be evaluated as follows:

1. Keep a list of the sites which have changed density since the previous time step.
2. Restrict either the  $i$  or the  $j$  sum to run only over values in the list, and add those contributions with weight 2.
3. Subtract afterward contributions with both sums restricted to run only over indices in the list, given weight 1.

If the  $\{\beta\}$  indices are a fraction  $f$  of the  $N^d$  index values, this algorithm speeds up the evaluation of  $S_q^{(k)}(r)$  by a factor of order  $f^{-1}$  for all time steps except the first one. (It is impractical to keep a list also of the  $\{\alpha\}$  sites, therefore the subtraction to avoid double-counting.)

### 2.3. Implementation and General Results

A  $256 \times 256$  lattice was used. Step-by-step output of the lattice state was displayed on a PC-AT computer. Number distributions of active sites were computed on a MicroVAX, while structure functions were computed on a CRAY X-MP. Transportable generators<sup>(12)</sup> for 32-bit computers and NAG Library generators<sup>(13)</sup> were used to obtain random numbers, on the CRAY (a 64-bit computer) only the latter ones. Runs were started with a random initial distribution of empty, filled, and active sites, determined by assigning density values continuously and randomly between 0 and  $2/(1 - p')$  and then truncating the values down to the nearest integer (corresponding to a fraction  $p'$  of the sites being active). The possibility  $p' \neq p$  was included. Optionally, runs could also be started with an inhomogeneous distribution intended to facilitate the formation of an extended front of active sites.

By visual observation, it was concluded that random self-activation with probability  $p$  cannot be used in the discrete model, if the aim is to get sustained fronts for small (but finite)  $p$  values. The random creation of active sites with subsequent nearest-neighbor activation will exhaust the density of filled sites, such that a density sufficient to allow for the formation of stable fronts will never build up. For the rest of this paper we will keep to the case with no self-activation.

Sustained and roughly straight (but fuzzy) fronts moving across the

lattice for 25,000 time steps or more without the emergence of a state with no active sites were obtained for  $p$  values down to  $p \approx 0.003$  with random initial conditions, and down to  $p \approx 0.0025$  with inhomogeneous initial conditions. Inhomogeneous initial conditions thus seem less essential than reported,<sup>(5)</sup> except of course that they may make a front develop in fewer time steps. Such fronts, once they were established, appeared to be quite stable configurations despite the tendency for formation of "plumes." This eliminated the need for sporadic random reactivation reported for smaller lattice sizes.<sup>(2)</sup> Cases of deactivation also appearing, for other seed values tried in the random number generator with the above-mentioned limiting  $p$  values, generally happened during the early time steps before a front had developed. For decreasing  $p$  there was a quite abrupt change to a situation where no seed values among those tried would result in a sustained front.

In the structure function calculations the algorithm described previously was used. The CPU time requirement for the calculation of  $S_2^{(1)}(r)$  on the CRAY was of the order of 30 min (without vectorization). For the

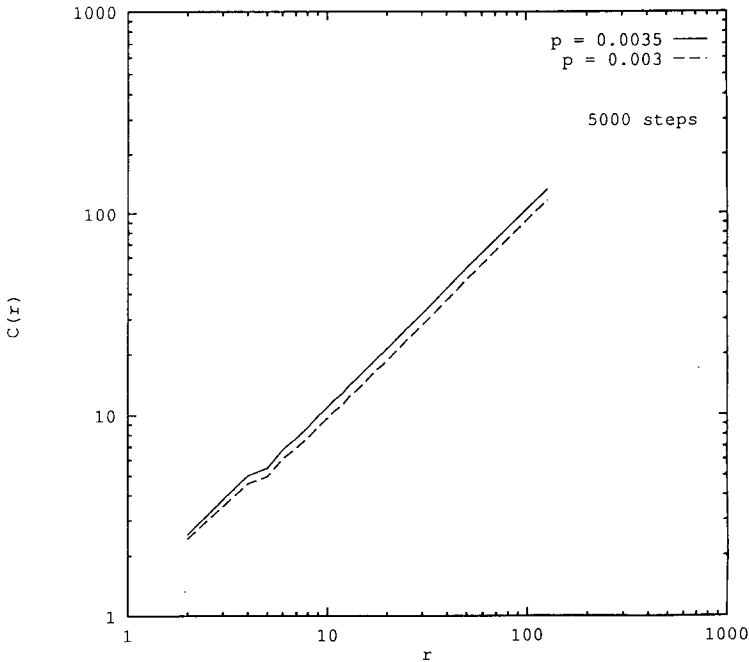


Fig. 1. Cumulative number distribution of active sites  $C(r)$  as a function of distance  $r$  from any active site. The curves are for  $p = 0.0035$  and  $p = 0.003$ . Averages over 5000 time steps are shown. Curves are drawn as straight lines between points for each integer  $r$ , therefore the wiggles for small  $r$ .

lowest  $p$  values, the number of sites changing density per time step was such that a factor of order 100 was gained by the calculation of each  $T_2^{(k)}(r)$  ( $k > 1$ ) compared to a calculation of  $S_2^{(k)}(r)$ .

### 2.4. Results for Number Distributions of Active Sites

Figure 1 shows cumulative number distributions of active sites as a function of distance  $r$  from any active site, with  $p = 0.003$  and  $p = 0.0035$ , for the case with no self-activation. The curves are averages over 5000 time steps, following an initial relaxation over 20,000 time steps. The closeness to unity of the fractal dimension ( $D = 0.987 \pm 0.003$  by least squares) follows trivially<sup>(5)</sup> from the straightness of the front. The “lacunarity” of the front makes  $D$  slightly smaller than 1. For a comparison, in Fig. 2 the curve for the very last time step ( $p = 0.0035$ ) is shown. The double sum (over a shell as well as average over center points) clearly leads to an improvement compared to the single-time-step results.

Particularly during the early time steps, before a stable front is established, there may be steps with very few active sites. With, for instance, 10,000 relaxation steps instead of 20,000, the curves therefore showed a

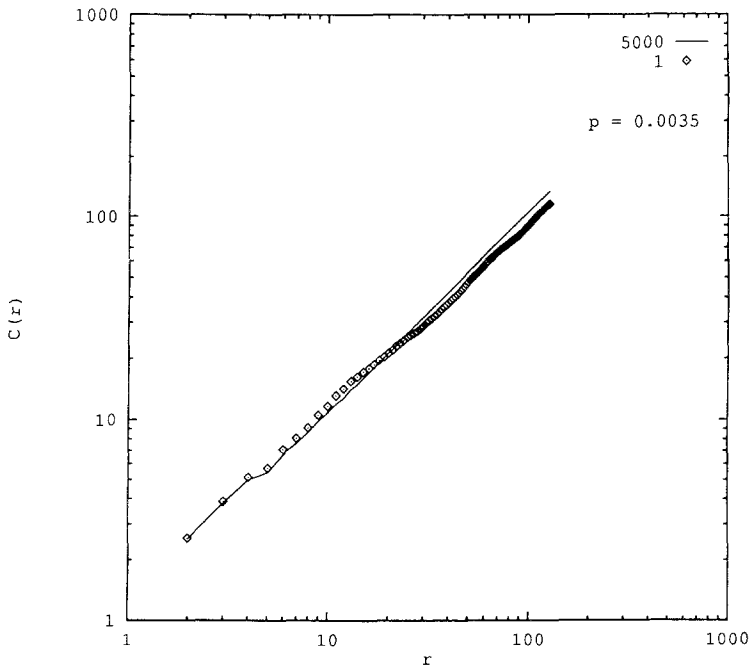


Fig. 2. Comparison of  $C(r)$  for one time step (the 25,000th), and  $C(r)$  averaged over 5000 steps (from 20,000 to 25,000). The curves are for  $p = 0.0035$ .

dependence on the seed and also on the generator chosen: Some runs led to curves with a smaller total number of active sites, but with nearly the same fractal dimension as shown above. That would be the effect of a large number of steps during which a straight front is being established, following a near deactivation.

## 2.5. Results for Structure Functions

Structure functions with  $q = 2, 4, 6,$  and  $8$  for  $p = 0.003$  are shown in Fig. 3, for the case with no self-activation. They are calculated by averaging over 100 time steps, following an initial relaxation over 24,900 steps. The much larger number of steps used for the continuous model<sup>(7)</sup> is only superficially more reliable, since there a large number was necessary because of the reliance on ergodicity (only one point per step was used as center point). The stability of the situation where a straight front moves across the lattice contributes also to the reliability of a calculation with a moderate number of steps included in the average. As a further check, Fig. 4 shows a comparison of the averaged  $q = 2$  and  $q = 4$  curves for  $p = 0.0035$  with the curves from the 25,000th time step only.

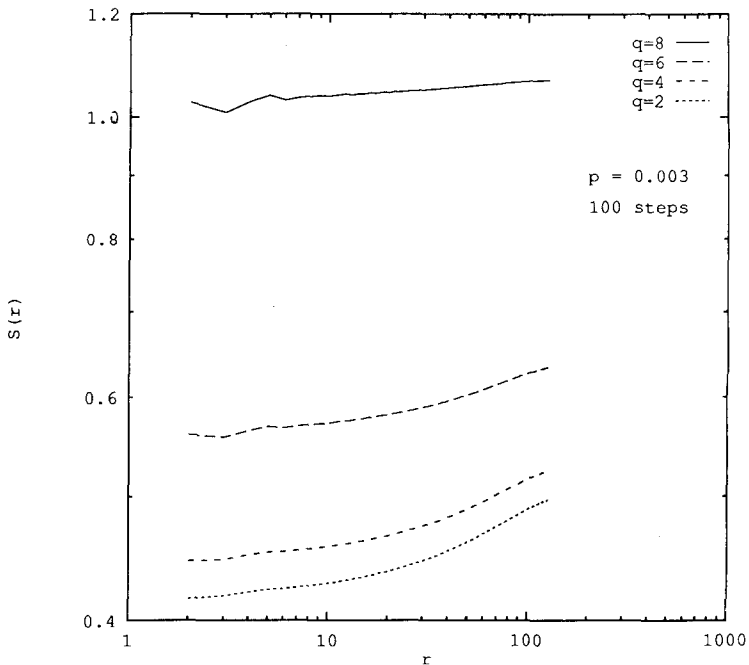


Fig. 3. Structure functions  $S_2(r)$ ,  $S_4(r)$ ,  $S_6(r)$ , and  $S_8(r)$  for  $p = 0.003$ . Averages over 100 time steps are shown. Curves are drawn as straight lines between points for each integer  $r$ .



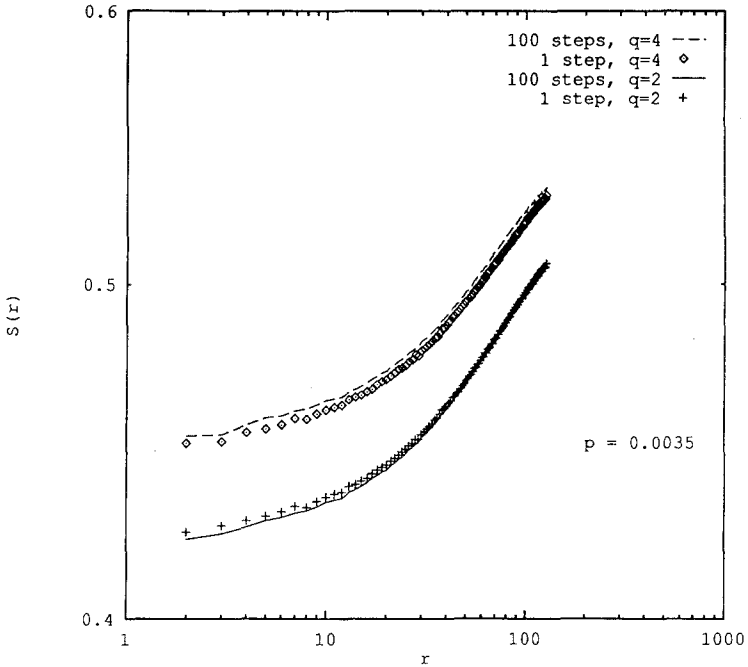


Fig. 4. Comparison of  $S_2(r)$  and  $S_4(r)$  for one time step (the 25,000th), and  $S_2(r)$  and  $S_4(r)$  averaged over 100 steps (from 24,900 to 25,000). The curves are for  $p = 0.0035$ .

The curves do not show scaling. For large  $r$  ( $\gg 10$ ), there may seem to be limited straight-line portions (though not with the slope dependence on  $q$  of the continuous model), but runs for  $p = 0.007$  merely resulted in a more distinct curvature at the large- $r$  and. Other checks excluded scaling in cases where a stable front had not yet developed, or with a straight front on the verge of disappearing because a too small  $p$  value had been chosen.

For  $a > b$ , one has  $S_a(r) > S_b(r)$ , while the continuous case had it the other way around. The reason is that here, a nonzero  $|\Delta n|$  is 1 or larger, while for the continuous case this difference could be smaller than unity.

### 3. DISCUSSION

The qualitative properties of the fronts and their fractal dimensions found here are consistent with earlier results on larger lattices.<sup>(5)</sup> The algorithm developed here has made possible a reliable evaluation of the structure functions. The same algorithm can be applied to the continuous case of ref. 7: Uniform growth at a pair of sites will not change their contribution to the structure function, so only the small number of sites activated

or deactivated per time step are of interest, allowing for a calculation for steps after the first one quite analogous to the one presented here.

For a front to develop after a random initialization, a number of time steps of the order of  $p^{-1}$  or larger is needed. Inclusion of the possibility for some random reactivation in the model, when (and only if) a state without active sites should occur<sup>(2)</sup> (which is a real problem for small lattice sizes), may therefore not be statistically insignificant. Activity-transfer models with and without reactivation, implemented on small lattices, may have significantly different dynamical properties.

Seed values for the limiting  $p$  values presented have been taken from the subset leading to 25,000 time steps or more without the emergence of total deactivation, for the generator and lattice size used. The necessity of imposing such a restriction is a shortcoming of the finite lattice approach. Since cases of total deactivation generally appeared prior to the emergence of an established front, it is assumed that the effect of the restriction amounts to the exclusion of transient effects.

It is not clear what role self-activation really played for the reported<sup>(7)</sup> continuous model results. If the fronts were mainly straight, the combination of lattice size and growth rate would seem to just make possible one front passage across the lattice without any sites being self-activated before the next arrival. If not, self-activation in the continuous model could lead to inherently different dynamics, and an expectation of similar scaling behavior would be unsubstantiated.

In the continuous case, the average density  $n$  behind a front will evidently increase roughly linearly with the distance  $y$  from the front, while in the discrete case, the average density behaves<sup>(5)</sup> like  $1 - e^{-py}$ . This may explain the difference in scaling behavior.

The observation of some curvature at the large- $r$  end of the structure function curves, becoming more distinct in runs with a larger  $p$  value, may indicate the presence of a saturation effect. Such indications of saturation over a distance of the order of the distance between fronts were also observed in the continuous case.<sup>(7)</sup> These effects are to be expected, since  $|n(\mathbf{x})| \leq 2$ , unlike the case of fluid turbulence, where there is no such bound. The power law in Eq. (3) will have a limited range of validity for a finite lattice, with the distance between fronts indicating the saturation distance.

Possibly, by an analogy with Ising-model criticality, the large- $r$  behavior in an SOC-type limit should exhibit a power-law decay of the correlation function,

$$S_q(r) \sim C - G_q(r) \quad (12)$$

$$G_q(r) \sim r^{-\eta(q)} \quad (13)$$

with, e.g.,

$$G_2(r) \equiv \langle [n(\mathbf{x}_0 + \mathbf{x}) - \langle n(\mathbf{x}_0 + \mathbf{x}) \rangle][n(\mathbf{x}_0) - \langle n(\mathbf{x}_0) \rangle] \rangle$$

and  $C$  a constant. However, the asymptotic limit is not well-defined, and may not show self-organized criticality.<sup>(5,6)</sup> The finite  $p$  (and  $N$ ) value of this work excludes an indication of the functional form of  $S_q(r)$  for asymptotically large lattices, where SOC behavior was originally<sup>(1,2)</sup> assumed to occur. (The restriction  $r_{\max} = N/2$  seems merely to exclude a region where at least the case without self-ignition would show an unavoidable noncritical saturation.) However, an eventual power-law scaling of  $S_q(r)$  for small  $r$  in the asymptotic limit would not be analogous to that observed in the continuous model, where a linear dependence of  $\zeta$  on  $q$  was found<sup>(7)</sup> for a considerable range in  $p$ , with the scaling form in Eq. (2) being visible down to  $r$  values of order 2 or 3.

#### 4. CONCLUSION

The discrete model, the basis for speculations about the role of self-organized criticality in some aspects of turbulence, does not have the scaling properties of the structure functions found in other models of turbulence. This lack of scaling may be related to the behavior of the average density as a function of distance from the front. It renders the continuous model better suited to explain certain aspects of turbulence. There are arguments, though, that no model with bounded variables should have the critical  $S_q(r)$  increasing algebraically with  $r$ . It also supports the claim that the discrete model does not show self-organized criticality.

Introduction of random self-activation results in a different behavior, without sustained fronts for small  $p$ . It is argued that opportunistic random reactivation can also result in statistically significant changes of the dynamics.

The algorithm developed in the present paper may facilitate future studies of the properties of these and similar models, in particular concerning their validity when applied to aspects of turbulence. It may also be more generally applicable for correlation calculations when only a small fraction of the sites in a matrix change their value per time step.

#### ACKNOWLEDGMENTS

The author would like to thank M. H. Jensen for a discussion, and P. Bak, P. Grassberger, and A. S. Pikovsky as well as an anonymous

referee for comments on the manuscript of this paper. Permission to use a CRAY X-MP on the quota of the Norwegian Research Council for Science and the Humanities is gratefully acknowledged.

## REFERENCES

1. P. Bak and K. Chen, The physics of fractals, *Physica D* **38**:5–12 (1989).
2. P. Bak, K. Chen, and C. Tang, A forest-fire model and some thoughts on turbulence, *Phys. Lett. A* **147**:297–300 (1990).
3. P. Bak, C. Tang, and K. Wiesenfeld, Self-organized criticality: An explanation of  $1/f$  noise, *Phys. Rev. Lett.* **59**:381–384 (1987).
4. K. Christensen, H. C. Fogedby, and H. J. Jensen, Dynamical and spatial aspects of sandpile cellular automata, *J. Stat. Phys.* **63**:653–684 (1991).
5. P. Grassberger and H. Kantz, On a forest fire model with supposed self-organized criticality, *J. Stat. Phys.* **63**:685–700 (1991).
6. P. Grassberger, Self-organized criticality, preprint (1990).
7. K. Chen, P. Bak, and M. H. Jensen, Weak chaos in a turbulent model, *Phys. Lett. A* **149**:207 (1990).
8. G. Paladin and A. Vulpiani, Anomalous scaling laws in multifractal objects, *Phys. Rep.* **156**:147–225 (1987).
9. M. H. Jensen, Personal communication (1990).
10. J. Finjord, Structure functions in a “forest-fire” model of turbulence, in *Spontaneous Formation of Space-Time Structures and Criticality*, T. Riste and D. Sherrington, eds. (Plenum Press, New York, 1991).
11. P. Grassberger and S. S. Manna, Some more sandpiles, Preprint WU B 90-5 (1990); *J. Phys.* (Paris), to appear.
12. W. H. Press, B. P. Flannery, S. A. Teukolsky, and W. T. Vetterling, *Numerical Recipes: The Art of Scientific Computing (FORTRAN Version)* (Cambridge University Press, Cambridge, 1989).
13. *NAG Fortran Library Manual*, Mark 14 (1990).